

# CRITICAL NUMBER OF SPACECRAFT IN LOW EARTH ORBIT: USING SATELLITE FRAGMENTATION DATA TO EVALUATE THE STABILITY OF THE ORBITAL DEBRIS ENVIRONMENT

Donald J. Kessler<sup>(1)</sup>, Phillip D. Anz-Meador<sup>(2)</sup>

<sup>(1)</sup>*Consultant, 507 S. Shadowbend, Friendswood, TX 77546, USA, Email: donkessler@swbell.net*

<sup>(2)</sup>*Viking Science and Technology Inc, 16821 Buccaneer Lane, Houston, TX 77058, USA, Email: panz-meador@vsti.com*

## ABSTRACT

Previous studies have concluded that fragments from random collisions in low Earth orbit will cause the orbital debris population to increase despite efforts to minimize the accumulation of debris. New data from the orbital history of fragments in space and the laboratory hypervelocity breakup of a payload more accurately confirms this conclusion. The conclusions are reached that the orbital debris environment for much of low Earth orbit is unstable and will seek a higher equilibrium even if no new debris is added to the environment. Some regions may be slightly above a runaway level, where no equilibrium is possible as long as the number of intact objects remains constant. The rate of increase for collision fragments is currently low, but would increase rapidly with increases in the intact population.

## 1. INTRODUCTION

A zero population growth of satellites in low Earth orbit might be achieved by a combination of limiting future explosions in Earth orbit, and by requiring future payloads and rocket bodies to reenter at the end of their operational life. However, if the number density of satellites is sufficiently high...above a "critical density"... then a zero population growth might not be possible because collisions between existing satellites could produce fragments at a rate faster than they are removed by atmospheric drag. A satellite population just above the critical density would experience a slowly increasing orbital debris environment, perhaps eventually growing to very high levels, despite efforts to minimize on-orbit explosions and orbital lifetimes.

Previous studies have attempted to define the level of critical density [1, 2, 3], and concluded that certain regions of low Earth orbit are already above the critical density. These studies were based on incomplete data. The studies contained assumptions that caused, in some cases, an under-estimate of the level of critical density, and in other cases, an over-estimate of the level. In addition, the term "critical density" was many times misunderstood. Some readers assumed the exceeding of critical density would result in an immediate exponential increase in the environment. This misunderstanding may

have resulted from an unclear definition of terms in some of the previous studies.

New data will be used in this paper to express a "critical number" of intact objects above a given altitude. While the resulting conclusions are not too different from previous studies, these conclusions are reached with greater confidence and a better understanding of their uncertainty.

## 2. FRAGMENT DATA

The fragments generated by a USAF test have produced a unique data set that can be used to help resolve the major uncertainties in determining critical density. The 850-kg satellite, known both as P-78 and Solwind, broke into 285 cataloged fragments after being hit with an approximately 16-kg projectile at 7 km/sec. This test was conducted September 13, 1985 at an altitude of 525 km...an altitude high enough that most of the fragments that were large enough to be cataloged were cataloged; therefore, the data set is nearly complete. In addition, the test was low enough that most of these fragments have decayed out of orbit, leaving a detailed time history. For example, the early January 1986 catalogue data contains 218 of the 285 total cataloged fragments. An additional 16 objects cataloged within the next year were changing orbital elements so slowly that their orbits in January 1986 could accurately be estimated. Therefore, from January 1986 to the present, we have a detailed decay history of 234 fragments. As of January 1998, only 8 of these fragments were still in orbit.

Using the orbital elements in this data set allows calculating the spatial density of collision fragments as a function of altitude at different times. Such a calculation requires no assumptions concerning area-to-mass, or velocity distribution of fragments, and does not require an accurate atmospheric drag model. This procedure allows for a much cleaner, less uncertain, determination of the fragment decay rates and how their orbit distributions affect various altitudes over time. The results can be applied to breakups at different altitudes by multiplying the time for the observed orbit changes by the ratio of atmospheric density at the desired altitude to the atmospheric density at 525 km. In the same way, the

results can be adjusted to reflect different solar activity conditions. The major assumption is that the P-78 fragments are typical of all collision fragments. This assumption must be tested, especially with respect to upper-stages.

Area-to-mass data and radar cross-section (RCS) data is also available for 202 of the P-78 fragments. The area-to-mass was determined from the decay history of the fragments. A measure of the debris diameter can be determined from the radar cross-section, under the assumption that the ground radar calibration tests, conducted to support the Haystack radar observations using collision fragments generated by ground hypervelocity tests, can be applied to the P-78 fragments. Under these assumptions, the mass of 202 of the 234-fragment sample can be calculated.

Ground hypervelocity tests have determined that for a collision to be catastrophic at 10 km/sec, the ratio of target mass to projectile mass should be less than 1250 [4]. This would mean that a fragment must have a mass greater than 0.68 kg in order to break up another satellite with the same 850-kg mass as P-78. The area-to-mass and debris diameter data of the P-78 fragments were used to calculate the mass of each of 202 fragments. The sum of these masses was found to be 1179 kg, or larger than the mass of the satellite. This could result from the uncertainty in the calculation of the mass of a single large fragment. However, the assumption will be made that this difference resulted from either an atmospheric density or radar cross-section systematic bias that resulted in the too-large calculated mass of all of the fragments. Therefore, all of the masses were reduced by a factor of 1.5, giving a total fragment mass of 786 kg, leaving 64 kg of fragments not counted. This procedure reduces the catalogued fragments in orbit in January 1986 to 68 fragments having a mass large enough to catastrophically break up another satellite the same size as P-78.

Fig. 1 is a plot of the spatial density of the 68 catalogued fragments larger than 0.68 kg just after the collision. These fragments are found much closer to the breakup altitude than the remaining, less massive, catalogued fragments. Similar plots were made for the time periods following the breakup thru 1998 when only 8 of these fragments were still in orbit. However, the most significant parameter to describe the effects of this breakup on other altitudes is the integral of these spatial density plots over time. Fig. 2 is the results of that integral.

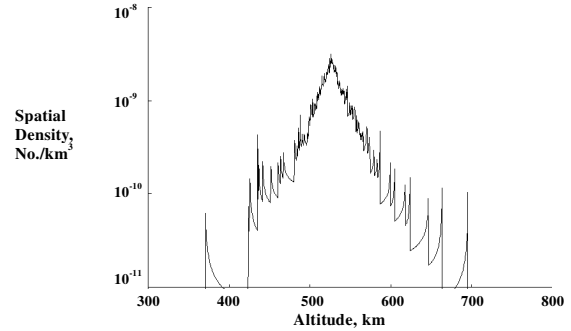


Fig. 1. Spatial Density of P-78 Catalogued Fragments Larger than 0.68 kg During January, 1986 (68 fragments)

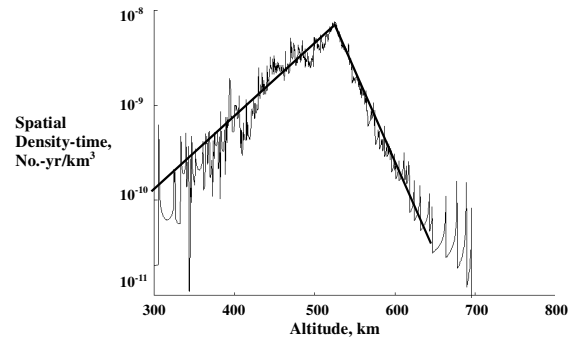


Fig. 2. Integral Spatial Density over time Sept 1985 to July 1998  $\int Sdt$  Masses larger than 0.68 kg

The altitude most affected is near the breakup altitude of 525 km. Fig. 2 illustrates that the effect on lower altitudes is inversely proportional to the atmospheric density, while the effect on higher altitudes is limited due to the small change in altitude of the fragments following the collision. The effects of breakups at 525 km from breakups at other altitudes can be approximated by letting the integral of its spatial density over time for altitudes lower than the breakup equal the line (or an extrapolation of the line) on the left side of Fig. 2; for altitudes higher than the breakup, the integral is approximated by a line parallel to the line on the right side of Fig. 2 and going through the breakup altitude. Consequently, collisions at higher altitudes are as important as collisions at a given altitude, and much more important to the given altitude than collisions at lower altitudes. In addition, the effects of collisions on all altitudes can be fairly accurately approximated by assuming that all of the breakup fragments are in circular orbits. If all of the fragments had been injected into circular orbits, the left side of the Fig. 2 would look nearly the same, while the right side would be a vertical line.

Fig. 3 is a plot of the log of the cumulative number of P-78 fragments as a function of log mass. The plot is close to linear for sizes larger than 2 kg, and follows a collision breakup model where number varies as the ratio of fragment mass to target mass to a power somewhere between  $-0.75$  and  $-0.85$ . This is as expected from most hypervelocity collision breakup models. For sizes smaller than 2 kg, the number does not increase as rapidly, suggesting that some of these fragments may not have been catalogued. Within the size interval between 2 kg and 0.68 kg, there are 31 fragments; 4 of these have diameters derived from their RCS of 15 cm and 2 of these have diameters of only 11 cm. Of all the 234 P-78 fragments, only 2 were determined to have a diameter less than 11 cm; a size of 11 cm is near the absolute smallest size that can be catalogued; sizes as small as 15 cm are difficult to catalogue. The fact that 11 to 15 cm objects were catalogued at sizes larger than 0.68 kg makes it probable that some fragments as small as 0.68 kg had an RCS corresponding to objects smaller than 11 cm. A metal sphere 11 cm in diameter would have to have a mass density of slightly less than 1 g/cc to have a mass of 0.68 kg. Consequently, it is possible that a dense metal or even an aluminum fragment could have a physical size of less than 11 cm and a mass greater than 0.68 kg. A linear extrapolation from sizes larger than 2 kg on Fig. 3 using a slope between  $-0.75$  and  $-0.85$  suggests that the number of fragments larger than 0.68 kg should be somewhere between 80 and 95.

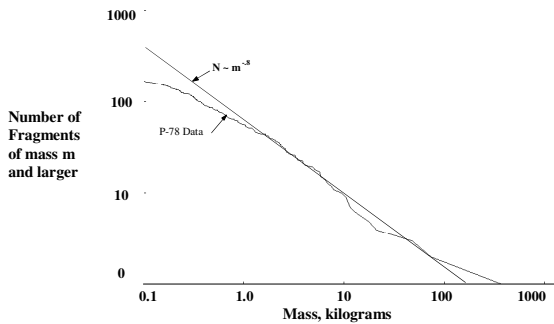


Fig. 3. Cumulative Number of P-78 Catalogued Fragments as a Function of Mass (January 1986)

The only ground hypervelocity breakup test of an actual satellite was the Transit/OSCAR satellite during the SOCIT series of hypervelocity tests. This test, sponsored by the Department of Defense, impacted a 150 g aluminum sphere at 6 km/sec into a 35.4 kg Navy navigation satellite [5]. The purpose of the test was to characterize in the laboratory the debris generated by a hypervelocity collision in space. The data analysis was completed with funding from NASA to more accurately characterize the resulting fragments. The mass of a fragment that would break up another satellite of Transit mass is  $34.5/1250 = 0.0276$  kg. The number of loose fragments of this size or larger was about 80. However,

the NASA-sponsored analysis concentrated on statistically analyzing the much larger number of fragments that had been captured in foam that lined the chamber. Some of the fragments larger than 0.0276 kg were captured in the foam. The NASA-sponsored analysis concluded that the number of fragments larger than 0.0276 kg should be about 90 to 100 [6], or about the same number of fragments larger than 1/1250 of the target mass suggested from the linear extrapolation of the P-78 data.

There is no fragmentation data on the hypervelocity breakup of upper-stages. However, there is data on upper-stage breakups resulting from explosions in orbit. Since nearly half of all intact objects are upper-stages, one should be aware of possible differences in the resulting collision fragment mass and area-to-mass distributions of upper-stages compared to payloads. The on-orbit explosion data may provide some clues. Area-to-mass data on 3,605 explosion fragments from 15 explosions of upper-stages in orbit was derived in the same manner as the area-to-mass data for the P-78 fragments. The diameter of these fragments was determined from the radar-cross section, just as it was with the P-78 fragments. These 15 events generated a total of 3,741 catalogued fragments and are believed to be representative of some of the more energetic explosions in Earth orbit; consequently, if explosions can duplicate a hypervelocity collision, these events might come closest. If so, a comparison of the upper stage fragments with the P-78 fragments indicates that the number of upper stage fragments capable of causing a catastrophic collision is less than the number of P-78 fragments, and these fragments reenter more quickly than the P-78 fragments. The implication of these findings will be discussed later.

From these data, the following conclusions are reached in Ref. [7]: 1. A catastrophic collision of a payload will produce about 90 fragments that are massive enough to catastrophically break up another payload of the same mass. 2. The orbits of these 90 fragments are sufficiently close to the orbit of the original payload to justify a model that assumes near-circular orbits for collision fragments. 3. The largest uncertainty in determining the stability of Low Earth Orbit is the lack of hypervelocity collision data for upper stages.

### 3. STABILITY MODEL

Most environment models average the environment over some volume of space. To obtain an accurate model that accounts for all of the debris, many volume elements are required. The model must then transfer the debris from one element to the other as the position of the debris changes. This usually leads to a complex model.

Another approach is to define the environment at a point in space by keeping track of only the rate that objects pass through that point. As will be seen, this approach can be particularly useful if that rate is the rate of orbital decay due only to atmospheric drag.

### 3.1 Model assumptions

Assume that above some altitude,  $h_1$ , the rate of breakups of intact spacecraft,  $dB/dt$ , is constant and producing fragments that decay through altitude  $h_1$ . Each collision is assumed to produce a time-dependent spatial density of  $S_1(t)$  at  $h_1$ . Then the average spatial density of fragments,  $S_B$ , is

$$S_B = dB/dt \int S_1(t) dt \quad (1)$$

Where Eq. 1 is integrated over the time it takes for the fragments to pass through  $h_1$ . The value of this integral could be obtained numerically from Fig. 2; however, as will be seen, because of the near-circular orbit of the fragments, a simpler analytical technique is available.

Assuming that the spatial density of intact spacecraft,  $S_i$ , and the spatial density of fragments large enough to catastrophically break up intact spacecraft,  $S_f$ , is constant within a volume of  $\Delta U$  above altitude  $h_1$ , then

$$dB/dt = S_i \sigma_i V \Delta U + S_i S_f \sigma_f V \Delta U \quad (2)$$

where it is assumed that when two intact objects collide, two breakups occur. The collision cross-section of two intact objects is  $\sigma_i$ , the collision-cross section between an intact object and a fragment is  $\sigma_f$ , and  $V$  is the relative velocity of collision, typically about 10 km/sec.

Finally, it will be assumed that the environment is in equilibrium. If the altitude of the volume above  $h_1$  is not too different than  $h_1$ , then the assumption that  $S_B = S_f$  is a fairly accurate one; however in general,  $S_f$  will always be greater than  $S_B$  when the environment is in equilibrium and the number of intact objects is constant with altitude. This could be handled by creating additional volume elements; however for the purposes of this paper the conservative assumption will be made that  $S_B = S_f$ .

### 3.2 Model development

In [8], the integral of spatial density over time for a circular orbit is expressed in terms of the rate of change of the orbital semi-major axis,  $da/dt$ . The integral for elliptical orbits is the same as for circular orbits times a weighting factor,  $W$ . Therefore, the integral in Eq. 1, assuming  $N_0$  fragments are produced by a single breakup, is

$$\int S_1(t) dt = \sum W / (4\pi a^2 da/dt) \quad (3)$$

where the summarization is for  $N_0$  fragments massive enough to break up an intact spacecraft. The value of  $W$  is 1 for circular orbits and is as high as 50 for certain highly-elliptical orbits. However for the slightly-elliptical orbits contained in the P-78 data, interpolation of the data in Kessler 1990 suggests that  $W$  would be less than 2, most likely near 1.3 to 1.5, just after the collision, and would approach 1 as the orbits decayed and circularized at lower altitudes.

The rate of change of the semi-major axis for circular orbits is derived from the drag force equation, an equation for the total energy of an orbit, and the equation in which energy loss is expressed as force through a distance. The drag force is equal to 1/2 of the product of the atmospheric density,  $\rho_a$ , the drag co-efficient  $C_D$  (approximately 2.2), the orbital velocity,  $V_o$ , squared, and the area-to-mass ratio,  $A/m$ . The total energy of an orbit is proportional to  $1/a$ .

The resulting equation is

$$da/dt = a \rho_a C_D V_o A/m \quad (4)$$

Combining Eqs. 3 and 4,

$$\int S_1(t) dt = N_0 W (m/A)_a / (4\pi a^3 V_o \rho_a C_D) \quad (5)$$

where  $(m/A)_a$  is the average  $m/A$  over the fragment  $m/A$  distribution. It is important to note that this is *not* the same as the average  $A/m$  over the  $A/m$  distribution.

Combining Eqs. 1 and 2 gives the equilibrium spatial density of fragments as

$$S_B = S_i^2 \sigma_i V \Delta U \int S_1 dt / (1 - S_i \sigma_f V \Delta U \int S_1 dt) \quad (6)$$

Notice that as  $S_i \sigma_f V \Delta U \int S_1 dt$  approaches 1,  $S_B$  goes to infinity. Also,  $S_i \Delta U = N_i$ , the number of intact objects above  $h_1$ . Therefore, after combining with Eq. 5, the critical number of intact objects above  $h_1$  producing a runaway environment is given by

$${}_R N_i = 4\pi a^3 V_o \rho_a C_D / (N_0 W (m/A)_a V \sigma_f) \quad (7)$$

where, if  $r_e$  is the radius of the earth,  $a = r_e + h_1$ .

The threshold for an "unstable" environment depends upon the current fragment population. The question posed is "given a current fragment population, will it increase due to random collision alone?" The question is answered by setting the current fragment population equal to  $S_B$  in Eq. 6, and solving for the value of  $S_i$  that produces an equilibrium equal to the current fragment population. The current fragment population can be defined as a factor,  $k$ , to be applied to the intact population. That is, let  $S_f = S_i/k = S_B$ . The critical

number of intact objects,  ${}_U N_i$ , corresponding to an unstable environment becomes

$${}_U N_i = {}_R N_i \sigma_f / (\sigma_f + k \sigma_i) \quad (8)$$

#### 4. RESULTS

Fig. 4 gives the spatial density of intact cataloged objects during February 1999.

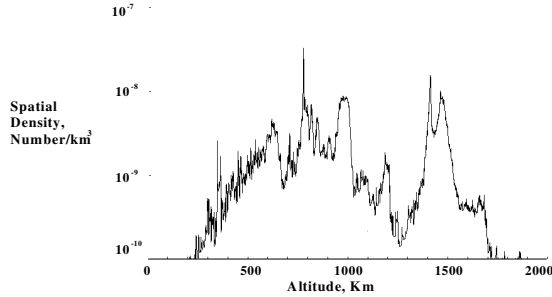


Fig. 4. Spatial Density of Intact Objects, Feb 1999

Four regions stand out as regions of high concentration of intact objects: (1) 570 km to 670 km; (2) 750 km to 860 km; (3) 920 km to 1020 km; and (4) 1350 km to 1550 km. Region 2 includes the Iridium constellation that causes the very sharp peak between 775 km and 780 km. The region below 670 km may be sufficiently low that atmospheric drag will remove fragments quickly so that this concentration may not be material; however, it will be included in the analysis since fragments generated in the regions above it will quickly decay into this region. Most fragments generated in region 3 that are massive enough to cause a catastrophic collision will require a few hundred years to decay into region 2, accelerated somewhat by collision scattering. Thus, the long-term stability of region 2 will be assumed to depend on region 3. However, the time for such fragments to decay from region 4 into region 3 is about 8,000 years; consequently, the region above 1350 km will be assumed to have no effect on the regions below 1000 km.

Below 1000 km, when payloads and upper-stages are looked at independently, they are found to show the same concentrations as Fig. 29, with the spatial density of each being about equal, except in region 4. In region 4, the concentration of intact objects is about 90% payloads and only 10% upper-stages.

Reference [7] concludes that the following values represent the most realistic values based on hypervelocity impact data and the current catalogue of objects in orbit for the regions of space below 1020 km:  $N_0 = 90$ ,  $(m/A)_a = 125 \text{ kg/m}^2$ ,  $\sigma_f = 14 \text{ m}^2$ ,  $\sigma_i = 53 \text{ m}^2$ ,  $W=1.1$ ,  $C_D = 2.2$ , and  $k=2$ . The value for  $(m/A)_a$  was obtained by averaging over the P-78  $m/A$  distribution; the values for  $\sigma$  were obtained by averaging over the known physical sizes of

intact objects and assuming a point size for fragments. Between 1350 km and 1550 km, where average intact sizes are smaller and fewer fragments are found, the following changes are necessary:  $(m/A)_a = 100 \text{ kg/m}^2$ ,  $\sigma_f = 2.3 \text{ m}^2$ ,  $\sigma_i = 6.6 \text{ m}^2$ , and  $k=10$ . At all altitudes, atmospheric densities were determined from NASA SP-8021 under the assumption of an average solar activity of 130. When combined with geomagnetic activity, this solar activity represents an exospheric temperature of 980 degrees Kelvin.

Fig. 5 gives the number of intact objects found between the given altitude and an altitude of 1020 km. This figure was derived from Fig. 4 by multiplying spatial density by volume to obtain the number, then summed between 1020 km and the given lower altitude. The figure illustrates that there are just over 1000 intact objects below 1020 km, and about 400 intact objects between 900 km and 1020 km. Also shown are the threshold numbers for both a runaway environment and for an unstable environment from Eqs. 7-8. Where the number of intact objects exceeds these thresholds, maintaining this environment of intact objects will cause the fragment population to increase. If the number of intact objects exceeds the unstable threshold, the increase will be either to a higher but eventually stable value; if the number of intact objects exceeds the runaway threshold, the environment will run away over an infinite amount of time to an infinite number of fragments. The region of space between 600 km and 1000 km is well above the unstable threshold and the region of space between 800 km and 970 km is above the runaway threshold.

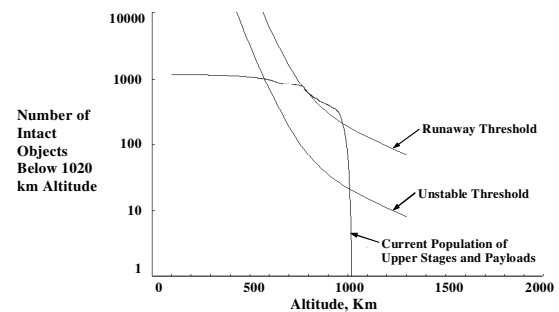


Fig. 5. Possible Regions of Instability Below 1020 km (Feb '99 Catalog)

#### 4.1 Upper stage explosion data implications

If the upper stage explosion data is indicative of the results of a hypervelocity collision, then these data indicate that the upper stage values for fragments would be  $N_0 = 50$  and  $(m/A)_a = 23 \text{ kg/m}^2$ . This would imply that payloads are nearly 10 times more important than upper stages in causing instabilities in the environment. If this were true, then upper stages could nearly be ignored. If they were ignored, since upper stages are larger than

payloads, average collision cross-sections would be reduced to  $\sigma_f = 4.9 \text{ m}^2$ ,  $\sigma_i = 18.6 \text{ m}^2$  for the region below 1020 km. Fig. 6 then represents a “best case” by ignoring the upper stages. Notice that although none of the environment below 1020 km is above the runaway threshold, certain parts are still above the unstable threshold. The actual regions of instability and runaway environment below 1020 km must be somewhere between that predicted in Fig. 5 and 6, and must await future data.

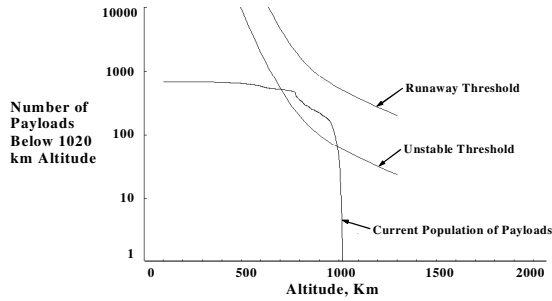


Fig. 6. “Best Case” Regions of Instability Below 1020 km (Feb ‘99 Catalog)

The same uncertainty does not exist for the region between 1350 km and 1550 km. This is because few rocket bodies are found within this region, and payloads dominate it. Fig. 7 gives the number of intact objects below 1550 km and the resulting thresholds for a runaway and unstable environment, using the smaller collision cross-sections and mass-to-area ratio, and the larger value of  $k$  previously defined for this region. The results predict that the region between 1300 km and 1420 km is above the runaway threshold and the entire region between 1000 km and 1500 km is above the unstable threshold.

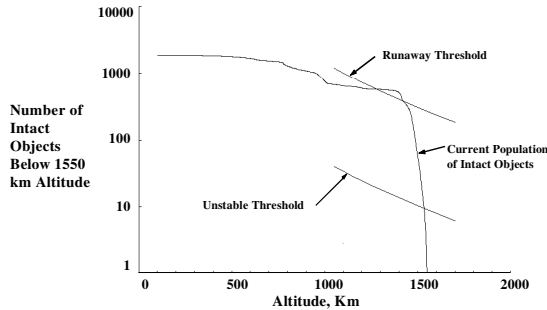


Fig. 7. Regions of Instability Below 1550 km (Feb ‘99 Catalog)

### 5. NUMERICAL MODEL

An existing “two-particle in a box” computer program was modified to use the same assumptions used to derive Eq. 6. This program does not explicitly look for any equilibrium or solve for critical density levels. Rather, the program calculates the number of collisions and resulting number of collision fragments generated in a 100-km altitude band as a function of time. An approximation in

the model calculates the “average” number of fragments generated per collision based on the expected frequency of intact-intact collisions and intact-fragment collisions. This approximation was required since the number of fragments per collision decreases as the number of fragments increases, since an “average” collision is more frequently an intact-fragment collision. The fragments were assumed to decay exponentially at a rate consistent with the decay rate of the P-78 fragments larger than 0.68 kg.

Fig. 8 gives the model predictions for the parameters used in Fig. 5, which predicts a runaway environment between 900 km and 1000 km. The number of fragments in Fig. 8 only doubles in about 100 years; however they are shown to continue to increase with time, without limits, as expected for a runaway environment. If the intact population were allowed to double, an order of magnitude increase in the fragment growth rate could result.

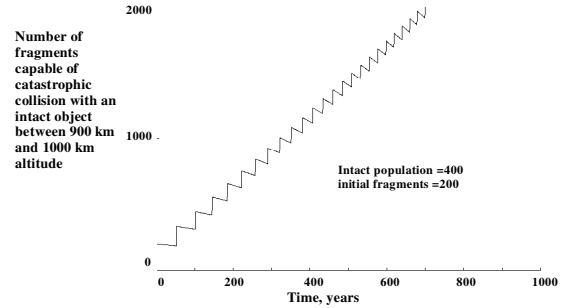


Fig. 8. Numerical Model Prediction for Region between 900 km and 1000 km. Assumes maintaining current population and eliminating explosions

Fig. 9 gives the model predictions for the parameter used in Fig. 6, which predicts an unstable environment between 900 km and 1000 km. This “best case” environment is shown to reach an equilibrium of about twice the current environment after a few thousand years.

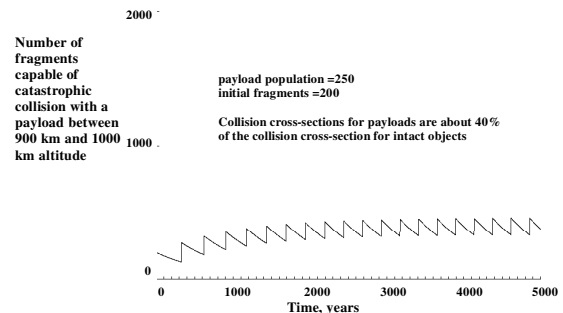


Fig. 9. Best Case Numerical Model Prediction for Region between 900 km and 1000 km. Assumes maintaining current population and eliminating explosions and upper stages contribute no fragments to the environment

Fig. 10 gives the model predictions for the parameters used in Fig. 7, which predicts a runaway environment

between 1400 km and 1500 km. While the rate of increase in fragments is very slow, this rate could be expected to continue as long as the intact population remains constant.

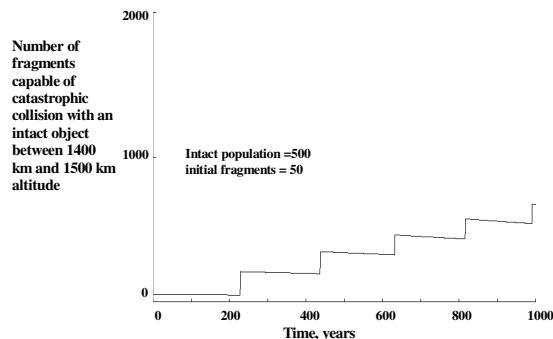


Fig. 10. Numerical Model Prediction for Region between 1400 km and 1500 km. Assumes maintaining current population and eliminating explosions

## 6. CONCLUSIONS

The USAF's intentional collision breakup of the P-78 satellite and the Department of Defense's laboratory hypervelocity breakup of a payload have provided the best data on the consequences of random collisions in Earth orbit. An analysis of the orbital decay history of the P-78 fragments leads to the conclusion that, if the current intact satellite population is maintained, large regions of low Earth orbit will be unstable. This instability would result from random collisions causing a slowly increasing fragment population, especially in the 700 km to 1000 km altitude region. For altitudes below 1000 km, the increase may level off and reach equilibrium over the next 1000 years or longer. However, if these hypervelocity tests are representative of upper-stage collisions as well, then an equilibrium environment in the region between 800 km and 970 km will never be reached.

The absence of hypervelocity breakup data for upper-stages is a critical limitation in determining which of these possibilities is most accurate, especially since most catastrophic collisions will involve an upper-stage, except in the region between 1350 km and 1550 km where small payloads dominate.

If the current intact population is allowed to continue to increase before being maintained at a particular level, the rate of increase in collision fragments can increase significantly. In practice, under these conditions and after some period of time, the intact population would be difficult to maintain because the fragment population would become too hazardous to continue space operations in low Earth orbit.

These results strongly support the implementation of current policy to limit the accumulation of intact objects

in Earth orbit and suggest that more actions may be required.

## 7. REFERENCES

1. Kessler D., "Collisional Cascading: The Limits of Population Growth in Low Earth Orbit", *Adv. Space Res.*, Vol. 11, No. 12, pp. 63-66, 1991.
2. Su Shin-Yi, "On Runaway Conditions of Orbital Debris Environment", *Adv. Space Res.*, Vol. 13, No. 8, pp (8)221-(8)224, 1993.
3. Anselmo L., Cordelli A., Farinella P., Pardini C., and Rossi A., "Modelling the Evolution of the Space Debris Population: Recent Research Work in Pisa", ESA SP-393, pp. 339-344, 1997.
4. McKnight D. S., Maher R. and Nagl, L., "Fragmentation Algorithms for Satellite Targets (FAST) Empirical Breakup Model, Version 2.0". Prepared for DOD/ DNA Orbital Debris Spacecraft Breakup Modeling Technology Transfer Program by Kaman Sciences Corporation, September 1992.
5. Hogg D.M., Cunningham T.M., Isbell W.M., "Final Report on the SOCIT Series of Hypervelocity Impact Tests", Wright Laboratory, Armament Directorate, Report No. WL-TR-93-7025, July 1993.
6. McKnight D., Johnson N., Fudge M. and Maclay T., "Analysis of SOCIT Debris Data and Correlation to NASA's Breakup Models", Kaman Sciences Corporation, prepared for NASA Johnson Space Center under contract number NAS 9-19215, July 1995.
7. Kessler D., "Critical Density of Spacecraft in Low Earth Orbit: Using Fragmentation Data to Evaluate the Stability of the Orbital Debris Environment", JSC #28949, LMSEAT # 33303, February 2000.
8. Kessler D., "Collision Probability at Low Altitudes Resulting from Elliptical Orbits", *Adv. Space Res.*, Vol. 10, No. 3-4, pp. (3)393-(3)396, 1990.